Simulation and Visualization of 3D-Spherical Distributions

S. Rao Jammalamadaka and Gyorgy Terdik

Abstract In this paper, we consider simulation and visualization of spherical distributions as well as plotting of densities and histograms on the sphere, in support of the dictum, "A picture is worth a thousand words." This is in many ways a companion paper to the recently published theoretical article by the authors on spherical harmonics (Jammalamadaka and Terdik in J Multivariate Anal 171:436–451, 2019 [1]). We provide computational algorithms to simulate several of the spherical models discussed there and provide alternate and improved methods in some cases. This allows a user to choose between alternate approaches for generating such random variates, and in depicting them via plots and histograms. The algorithms are made available in a MATLAB package titled "3D-Directional Statistics, Simulation, and Visualization" abbreviated **3D-Directional-SSV** which is available at MATLAB, File Exchange, and also posted on GitHub. This work is especially appropriate in this volume celebrating Florence Nightingale, the progenitor of what we now call the rose diagram in two dimensions.

1 Introduction

Vector space representation provides a very efficient method for displaying and analyzing spherical data, both in the natural world and for the theoretical framework. Further practical exploration and analysis in this area depend on related software and associated algorithms. We consider spherical distributions on the surface of the unit sphere $\mathbb{S}_2$ embedded in $\mathbb{R}^3$, facilitating the validation and testing of the theory presented in Rao and Gy [1] and related papers. We develop the necessary computational tools to achieve this goal and produce what we believe will be a valuable resource

S. R. Jammalamadaka (✉)
Department of Statistics and Applied Probability, University of California, Santa Barbara, USA
e-mail: rao@pstat.ucsb.edu; sreenivas@ucsb.edu

G. Terdik
Faculty of Informatics, University of Debrecen, Debrecen, Hungary
e-mail: terdik.gyorgy@inf.unideb.hu

for scientists interested in statistical analysis of directional data in 3 dimensions. These tools are provided in the form of a MATLAB package titled "3D-Directional Statistics, Simulation, and Visualization" abbreviated **3D-Directional-SSV**.

We start with a summary of what we call the Generalized Fisher–Bingham (**GFB**) family of distributions and point out the structure and relationship between various subfamilies therein. We review and reconsider earlier work by Wood [2], Kent [3], and a more recent R-package by Kent et al. [4] for the simulation of selected distributions belonging to this **GFB** family. Our MATLAB package, "**3D-Directional-SSV**," makes necessary modifications for our specific context, while taking advantage of recent developments in software routines. An impetus for this computational exploration is in support of the theoretical work developed in Jammalamadaka and Terdik [1]. Besides covering the entire **GFB** family of distributions, our work provides visualization and simulation tools for new spherical distributions characterized by their spherical harmonics as discussed there.

The potential research applications and uses of this software are many and yet to be fully explored. Such visualization of spherical models and plotting of densities and histograms is made possible on the surface of the unit sphere in high relief, as opposed to the more typical *heatmap* representation. The topographical composition of the plots (density, simulated data, and histogram) provides a much clearer graphical representation.

We note here that an earlier work by Gatto [5] discusses several generalizations of the von Mises–Fisher distribution to higher dimensions including for dimension greater than 3, while providing spherical plots for 3 dimensions. However visualization and plotting of such models in more than 3 dimensions appear to be a difficult task, except for some selected cross sections of such models, and will be looked into elsewhere.

Sect. 2 provides a detailed account of the **GFB** family of distributions and their interrelationships, along with a schematic diagram of these relationships between **GFB** subfamilies. We then describe the background theory and connections between the various subfamilies, as it will be needed for the simulations that come later. Section 3 describes how a histogram for a random sample of observations on the unit sphere $\mathbb{S}_2$, may be plotted. Section 4 includes various algorithms for the simulations and visualization, along with some useful explanations.

Besides the MATLAB package **3D-Directional-SSV** which is available at MATLAB, File Exchange, and on GitHub, a supplement available by request from the authors contains the MATLAB Scripts and descriptions of the various algorithms used here.

2 GFB Family of Distributions and Their Interrelationships

Let

$$\widetilde{\underline{x}} = \widetilde{\underline{x}}(\vartheta, \varphi) = (\sin\vartheta\cos\varphi, \sin\vartheta\sin\varphi, \cos\vartheta)^\top,$$

represent a point on the surface of the unit sphere $\mathbb{S}_2$ in $\mathbb{R}^3$, with colatitude $\vartheta \in [0, \pi]$ and longitude $\varphi \in [0, 2\pi]$. We consider density functions $f\left(\widetilde{\underline{x}}\right)$ on such an $\mathbb{S}_2$.

We shall use 2 alternate notations for a density viz. $f\left(\widetilde{\underline{x}}\right)$ and $f(\vartheta, \varphi)$, the main difference between them being that $f\left(\widetilde{\underline{x}}\right)$ corresponds to the Lebesgue measure $Q\left(d\widetilde{\underline{x}}\right) = \sin\vartheta\, d\vartheta\, d\varphi$, while $f(\vartheta, \varphi)$ includes $\sin\vartheta$ in it, and corresponds to the measure $d\vartheta\, d\varphi$ on the set $(\vartheta, \varphi) \in [0, \pi] \times [0, 2\pi]$. For instance, if X is a random unit vector which is distributed uniformly on $\mathbb{S}_2$ (see [6], Sect. 9.3.1), then the *Uniform* density $f\left(\widetilde{\underline{x}}\right) = 1/4\pi$, $\widetilde{\underline{x}} \in \mathbb{S}_2$ is constant, while the same uniform density becomes

$$f(\vartheta, \varphi) = \frac{1}{4\pi}\sin\vartheta,$$

in terms of the coordinates (Θ, Φ), making Θ and Φ independent, with Θ distributed as $(\sin\vartheta)/2$ on $[0, \pi]$ and Φ is uniform on $[0, 2\pi]$.

An important consequence of this dual representation, in connection with the simulation of random variates on the unit sphere $\mathbb{S}_2$ is the following. One may simulate a random variate (Θ, Φ) according to the density $f(\vartheta, \varphi)$ and then use $\widetilde{X}(\Theta, \Phi) = (\sin\Theta\cos\Phi, \sin\Theta\sin\Phi, \cos\Theta)^\top$ to get a random point on $\mathbb{S}_2$, or simulate directly a random variate $\widetilde{\underline{X}} \in \mathbb{S}_2$ according to the density $f\left(\widetilde{\underline{x}}\right)$.

A distribution is considered *uni-, bi-,* and *multimodal* if it has one, two, or more modes. In case there are two modes at the opposite ends; i.e., there is an axis joining the two modes, we call this a *bipolar* distribution. If the mass is concentrated around the main circle, it will be called a *girdle distribution*. Examples that follow, will make these notions clear.

One of the earliest and commonly used models for spherical data is the (unimodal) von Mises–Fisher distribution [7] which can be extended to an antipodally symmetric model; i.e., the density has same values antipodal points, as given by the Dimroth [8] and Watson [9]. Such antipodally symmetric models were further generalized by Bingham [10]. Such models belong to the exponential family, and we refer to them as the "Generalized Fisher–Bingham Family" and label them the **GFB** family. It has several subfamilies depending on the number of parameters. Figure 1 provides a schematic of the relationships between different members of the **GFB** family of distributions. The **GFB** family of spherical distributions containing 8 parameters, labeled **GFB**$_8$, is given by the density (cf. [10]),

$$f_8\left(\widetilde{\underline{x}}; \widetilde{\underline{\mu}}_0, \kappa, A\right) \cong \exp\left(\kappa\widetilde{\underline{\mu}}_0 \cdot \widetilde{\underline{x}} + \widetilde{\underline{x}}^\top A\widetilde{\underline{x}}\right), \tag{1}$$

where $\cong$ denotes equality up to a multiplicative constant and where $\widetilde{\underline{\mu}}_0 \in \mathbb{S}_2$, A is a symmetric 3×3 matrix and $\widetilde{\underline{\mu}}_0 \cdot \widetilde{\underline{x}}$ denotes the usual inner product. Matrix A has the form $A = MZM^\top$, where $M = \left[\widetilde{\underline{\mu}}_1, \widetilde{\underline{\mu}}_2, \widetilde{\underline{\mu}}_3\right]$ is an orthogonal matrix and $Z = \text{diag}(\zeta_1, \zeta_2, \zeta_3)$ is a diagonal matrix.

For an arbitrary constant ζ one can check that changing the matrix A to $A_1 = MZ_1M^\top$ in (1) with
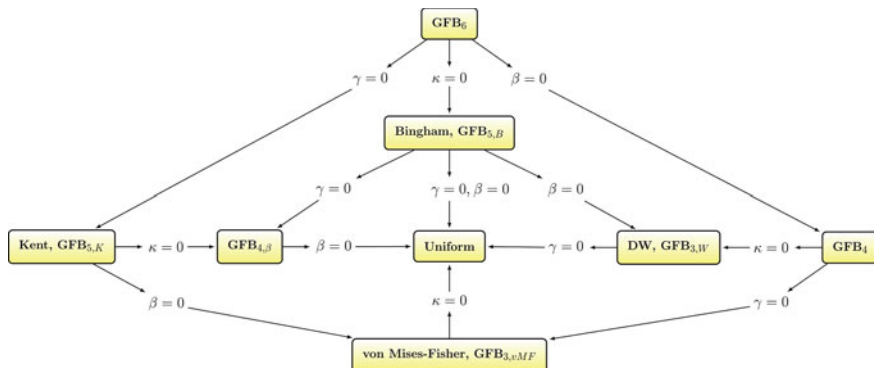
Fig. 1 Relationships between **GFB** family of distributions

$$Z_1 = \text{diag}\left(\zeta_1 - \zeta, \zeta_2 - \zeta, \zeta_3 - \zeta\right), \tag{2}$$

the density (1) will remain the same. Therefore, in order to avoid identifiability problems it is necessary to impose some constraints. Setting $\zeta = \left(\zeta_1 + \zeta_2 + \zeta_3\right)/3$, one usually assumes that

$$\text{tr}\left(A\right) = \zeta_1 + \zeta_2 + \zeta_3 = 0. \tag{3}$$

Under this assumption, $\zeta_3 = -\zeta_1 - \zeta_2$, and Z is determined by the two parameters ζ_1 and ζ_2.

The unique set of parameters of the density (1) has a cardinality of 8. These are

1. the parameter κ,
2. two angles $\left(\vartheta_\mu, \varphi_\mu\right)$, which define $\underline{\widetilde{\mu}}_0 = \left(\sin \vartheta_\mu \cos \varphi_\mu, \sin \vartheta_\mu \sin \varphi_\mu, \cos \vartheta_\mu\right)^\top$,
3. two eigenvalues ζ_1, ζ_2, of A, and
4. three Euler angles which define the orthogonal matrix M, considered as a rotation matrix.

Using the terminology as in [3], this is the **GFB$_8$** model and has the density (1) of the form,

$$f_8\left(\underline{\widetilde{x}}; \underline{\widetilde{\mu}}_0, \kappa, \zeta_1, \zeta_2, M\right) \cong \exp\left(\kappa \underline{\widetilde{\mu}}_0 \cdot \underline{\widetilde{x}} + \sum_{k=1}^{3} \zeta_k \left(\underline{\widetilde{\mu}}_k \cdot \underline{\widetilde{x}}\right)^2\right).$$

If we set $\zeta = \left(\zeta_1 + \zeta_2\right)/2$ in (2), an equivalent form of (1) can be obtained with density given by

$$f_8\left(\underline{\widetilde{x}}; \kappa, \beta, \gamma, \underline{\widetilde{\mu}}_0, M\right) \cong \exp\left(\kappa \underline{\widetilde{\mu}}_0 \cdot \underline{\widetilde{x}} + \gamma \left(\underline{\widetilde{\mu}}_3 \cdot \underline{\widetilde{x}}\right)^2 + \beta \left(\left(\underline{\widetilde{\mu}}_1 \cdot \underline{\widetilde{x}}\right)^2 - \left(\underline{\widetilde{\mu}}_2 \cdot \underline{\widetilde{x}}\right)^2\right)\right).$$
$$\tag{4}$$

In this paper, *we shall consider densities in this particular form* (4), wherein the three parameters κ, β, and γ satisfy the following:

Condition The parameters of the density (4) satisfy: $\kappa \in \mathbb{R}$, $\beta \geq 0$, $\gamma \in \mathbb{R}$. $\square$

Remark 1 Notice that we are allowing for $\kappa \in \mathbb{R}$; however a sign change of κ is equivalent to changing either $\widetilde{\underline{\mu}}_0$ to $-\widetilde{\underline{\mu}}_0$, or $\widetilde{\underline{x}}$ to $-\widetilde{\underline{x}}$, since the quadratic form in the density (4) is invariant under transformation $\widetilde{\underline{x}}$ to $-\widetilde{\underline{x}}$. The sign change of κ will only interchange the hemispheres, so that one may consider the absolute value $|\kappa|$ as the true parameter of concentration. If $\kappa \leq 0$, then

$$f_8\left(\widetilde{\underline{x}}; \kappa, \beta, \gamma, \widetilde{\underline{\mu}}_0, M\right) = f_8\left(-\widetilde{\underline{x}}; -\kappa, \beta, \gamma, \widetilde{\underline{\mu}}_0, M\right)$$
$$= f_8\left(\widetilde{\underline{x}}; -\kappa, \beta, \gamma, -\widetilde{\underline{\mu}}_0, M\right).$$

In terms of colatitude and longitude one can use the transformation $\vartheta \to \pi - \vartheta$, and $\varphi \to \varphi + \pi$, for getting $\widetilde{\underline{x}} \to -\widetilde{\underline{x}}$.

Although we discuss the most general **GFB**$_8$ distribution here for completeness, in practice we would be able to make use of convenient restrictions, as we do in the next section, which will allow us to reduce the number of parameters, without significant loss of generality or flexibility.

2.1 Model GFB$_6$

We apply a restriction on the **GFB**$_8$ by setting either $\widetilde{\underline{\mu}}_0 = \widetilde{\underline{\mu}}_3$, or by assuming $\widetilde{\underline{\mu}}_0$ is collinear to $\widetilde{\underline{\mu}}_3$ in the model (4). In this way, we can reduce the number of parameters by two, i.e., by the two angles $(\vartheta_{\mu_0}, \varphi_{\mu_0})$, which define $\widetilde{\underline{\mu}}_0$. The resulting **GFB**$_6$ model has a density given by,

$$f_6\left(\widetilde{\underline{x}}; \kappa, \beta, \gamma, M\right) \cong \exp\left(\kappa\widetilde{\underline{\mu}}_3 \cdot \widetilde{\underline{x}} + \gamma\left(\widetilde{\underline{\mu}}_3 \cdot \widetilde{\underline{x}}\right)^2 + \beta\left(\left(\widetilde{\underline{\mu}}_1 \cdot \widetilde{\underline{x}}\right)^2 - \left(\widetilde{\underline{\mu}}_2 \cdot \widetilde{\underline{x}}\right)^2\right)\right).$$
(5)

We can split up the rotation, which transforms the original xyz system into the orthogonal system defined by $M = \left[\widetilde{\underline{\mu}}_1, \widetilde{\underline{\mu}}_2, \widetilde{\underline{\mu}}_3\right]$, into two separate rotations. The first rotation, $G_{\widetilde{\underline{\mu}}_3, \widetilde{\underline{N}}}$, will rotate the north pole $\underline{\widetilde{N}} = (0, 0, 1)^\top$ to $\widetilde{\underline{\mu}}_3$, i.e., $G_{\widetilde{\underline{\mu}}_3, \underline{\widetilde{N}}}\underline{\widetilde{N}} = \widetilde{\underline{\mu}}_3$. Such a rotation $G_{\widetilde{\underline{\mu}}_3, \underline{\widetilde{N}}}$ can be constructed in the following way. The vectors $\underline{\widetilde{N}}$ and $\widetilde{\underline{\mu}}_3$ define a plane with normal vector $\underline{\widetilde{N}} \times \widetilde{\underline{\mu}}_3$ (cross product). Now, let $\underline{\widetilde{N}} \times \widetilde{\underline{\mu}}_3$ be the axis of rotation and rotate $\underline{\widetilde{N}}$ to $\widetilde{\underline{\mu}}_3$. This rotation depends solely on $\widetilde{\underline{\mu}}_3$, i.e., via the two angles ϑ_μ and φ_μ of $\widetilde{\underline{\mu}}_3$. When we rotate the sphere by $G_{\widetilde{\underline{\mu}}_3, \underline{\widetilde{N}}}$, the plane of rotated x- and y-axes coincides with the plane defined by $\widetilde{\underline{\mu}}_1$ and $\widetilde{\underline{\mu}}_2$, since $\widetilde{\underline{\mu}}_3$ is now perpendicular to both planes. Next, using $\widetilde{\underline{\mu}}_3$ as the axis of rotation, we rotate

the sphere by an angle $\psi \in [0, 2\pi]$ such that $\widetilde{\underline{\mu}}_1$ coincides with the rotated x-axis, and $\widetilde{\underline{\mu}}_2$ coincides with the rotated y-axis. We will denote this rotation by $G_{\widetilde{\underline{\mu}}_{1,2},xy}$. These three angles ϑ_μ, φ_μ and ψ, called the Euler angles, characterize the rotation from the original orthogonal system to the orthogonal system $M = \left[\widetilde{\underline{\mu}}_1, \widetilde{\underline{\mu}}_2, \widetilde{\underline{\mu}}_3 \right]$.

Note here that the rotations from one system to another are not unique and during simulations we shall apply the above rotation for the densities, their simulations, and histograms.

The six parameters of Model **GFB**$_6$ are then κ, β, γ and M. If $\widetilde{\underline{\mu}}_3$ is known we can apply $G_{\widetilde{\underline{\mu}}_3, \widetilde{\underline{N}}}$ and rotate it to the north pole $\widetilde{\underline{N}}$ and (5) will have the form

$$f_6 \left(\widetilde{\underline{x}}; \kappa, \beta, \gamma, \widetilde{\underline{N}}, \psi \right) \cong \exp \left(\kappa \widetilde{x}_3 + \gamma \widetilde{x}_3^2 + \beta \left(\left(\widetilde{\underline{\mu}}_1^1 \cdot \widetilde{\underline{x}} \right)^2 - \left(\widetilde{\underline{\mu}}_2^1 \cdot \widetilde{\underline{x}} \right)^2 \right) \right),$$

where again, $\widetilde{\underline{x}} = (\widetilde{x}_1, \widetilde{x}_2, \widetilde{x}_3)$, and $\widetilde{\underline{\mu}}_k^1$ are the transformed $\widetilde{\underline{\mu}}_k$, by $G_{\widetilde{\underline{\mu}}_3, \widetilde{\underline{N}}}$. Applying $G_{\widetilde{\underline{\mu}}_{1,2},xy}$, the density in the new coordinate system is

$$f_6 \left(\widetilde{\underline{x}}; \kappa, \beta, \gamma, \widetilde{\underline{N}}, 0 \right) \cong e^{\kappa \widetilde{x}_3 + \gamma \widetilde{x}_3^2 + \beta \left(\widetilde{x}_1^2 - \widetilde{x}_2^2 \right)} = e^{\kappa \cos \vartheta + \gamma \cos^2 \vartheta + \beta \sin^2 \vartheta \cos 2\varphi}.$$

For simplicity, if $\widetilde{\underline{\mu}}_3 = \widetilde{\underline{N}}$ and $\psi = 0$, we may introduce the notation

$$f_6 \left(\widetilde{\underline{x}}; \kappa, \beta, \gamma \right) = f_6 \left(\widetilde{\underline{x}}; \kappa, \beta, \gamma, \widetilde{\underline{N}}, 0 \right),$$

and call it the *canonical form*.

The mean direction $\widetilde{\underline{\mu}}$ of the model **GFB**$_6$ given by (5), is characterized by a constant times $\kappa M^\top \widetilde{\underline{N}}$, in particular if $\kappa = 0$, then $\widetilde{\underline{\mu}}$ is undefined ($\widetilde{\underline{\mu}} = 0$, see [1] for details).

Remark 2 The Model **GFB**$_6$ is rotationally symmetric with respect to the axis $\widetilde{\underline{N}}$ if and only if $\beta = 0$ ([1]). An example of rotational symmetry of **GFB**$_6$, when $\beta \neq 0$, is given in Remark 5, where the axis of rotation is the y-axis.

From now on we consider densities in the canonical form and simulate random variates when $\widetilde{\underline{\mu}}_3 = \widetilde{\underline{N}}$ and $\psi = 0$. If we are given a matrix of rotation $M = \left[\widetilde{\underline{\mu}}_1, \widetilde{\underline{\mu}}_2, \widetilde{\underline{\mu}}_3 \right]$, then we apply this rotation as the last step of the simulation. As we have seen above, this rotation can be given by $\widetilde{\underline{\mu}}_3$ and angle ψ, such that we rotate $\widetilde{\underline{N}}$ to $\widetilde{\underline{\mu}}_3$, then use $\widetilde{\underline{\mu}}_3$ as the axis of rotation and rotate the sphere by angle ψ. This is the reverse rotation from what we described above. Formally, we apply the product of the two rotations $G_{\widetilde{\underline{N}}, \widetilde{\underline{\mu}}_3} \cdot G_{xy, \widetilde{\underline{\mu}}_{1,2}}$, noting that the product of the two rotations $G_{\widetilde{\underline{\mu}}_3, \widetilde{\underline{N}}} \cdot G_{\widetilde{\underline{\mu}}_{1,2},xy}$ is again a rotation.

Considering the density by applying the transformation $x = \cos \vartheta$, as is done in [2],

$$\widetilde{x}_1 = \sqrt{1 - x^2} \cos \varphi, \ \widetilde{x}_2 = \sqrt{1 - x^2} \sin \varphi, \ \widetilde{x}_3 = x, \tag{6}$$

with the derivative $-\mathrm{d}x = \sin\vartheta\,\mathrm{d}\vartheta$, we obtain what we will hereafter refer to as the *basic* form of the density f_6, given by

$$
\begin{aligned}
g_6\left(x, \varphi; \kappa, \beta, \gamma\right) &\cong \mathrm{e}^{\kappa x + \gamma x^2 + \beta\left(1 - x^2\right)\cos 2\varphi} \\
&= \mathrm{e}^{\beta\left(1 - x^2\right)\cos 2\varphi}\mathrm{e}^{\kappa x + \gamma x^2}.
\end{aligned}
\tag{7}
$$

This is the joint density in x and φ, and can be considered as the product of two densities, where $\exp\left(\kappa x + \gamma x^2\right)$ is a density in x, and $\exp\left(\beta\left(1 - x^2\right)\cos 2\varphi\right)$ is the conditional density of Φ given X. More precisely

$$
g_6\left(x, \varphi; \kappa, \beta, \gamma\right) = g_{\Phi|X}\left(\varphi|x; \beta\right)g_{6,X}\left(x; \kappa, \gamma\right),
$$

where

$$
g_{6,X}\left(x; \kappa, \beta, \gamma\right) \cong \exp\left(\kappa x + \gamma x^2\right)\int_0^{2\pi} \mathrm{e}^{\beta\left(1 - x^2\right)\cos 2\varphi}\mathrm{d}\varphi = I_0\left(\beta\left(1 - x^2\right)\right)\mathrm{e}^{\kappa x + \gamma x^2}.
$$

It follows from (7) that

$$
g_{\Phi|X}\left(\varphi|x; \beta\right) \cong \mathrm{e}^{\beta\left(1 - x^2\right)\cos 2\varphi}.
\tag{8}
$$

The densities $g_{6,X}\left(x; \kappa, \beta, \gamma\right)$ and $g_{\Phi|X}\left(\varphi|x; \beta\right)$ will be called the *marginal density*, and the *conditional density* respectively. The conditional density $g_{\Phi|X}$ remains the same throughout this paper, and therefore we do not refer to the specific subfamily to which it corresponds.

Remark 3 Given $X = x$, the conditional density (8) follows vMF distribution (see Sect. 2.6) with parameter $\beta\left(1 - x^2\right)$ and is a function of 2φ. It is worth mentioning that $g_{\Phi|X}\left(\varphi|x; \beta\right)$ is not a vMF distribution on the unit sphere $\mathbb{S}_2$ since the factor $(\sin 2\varphi)$ is missing from (8), but it **is** vMF distributed on the unit circle $\mathbb{S}_1$.

We now consider special cases of Model $\mathbf{GFB}_6$, when one of the basic parameters κ, β, γ is zero. Although the densities in these cases follow directly from the densities f_6 and g_6, we list them individually in order of decreasing complexity. The algorithms for the simulation of these models will be given in Sect. 4, in reverse order, incrementally increasing the number of parameters and the model complexity.

2.2 Kent Model $\mathbf{GFB}_{5,K}$

Let $\gamma = 0$ in (5) so that the number of parameters in $f_6\left(\widetilde{x}; \kappa, \beta, \gamma, M\right)$ is reduced by one (i.e., by parameter γ), and takes the form

$$f_5\left(\widetilde{\underline{x}}; \kappa, \beta, M\right) \cong \exp\left(\kappa\widetilde{\underline{\mu}}_3 \cdot \widetilde{\underline{x}} + \beta\left(\left(\widetilde{\underline{\mu}}_1 \cdot \widetilde{\underline{x}}\right)^2 - \left(\widetilde{\underline{\mu}}_2 \cdot \widetilde{\underline{x}}\right)^2\right)\right), \qquad (9)$$

which defines the five parameter model $\mathbf{GFB}_{5,K}$. The five parameters are κ, β, and M, with the canonical form

$$f_5\left(\widetilde{\underline{x}}; \kappa, \beta\right) \cong e^{\kappa\widetilde{x}_3 + \beta\left(\widetilde{x}_1^2 - \widetilde{x}_2^2\right)}.$$

In terms of ϑ and φ

$$f_5\left(\widetilde{\underline{x}}; \kappa, \beta\right) \cong e^{\kappa\cos\vartheta + \beta\sin^2\vartheta\cos 2\varphi}, \qquad (10)$$

(see [2]). If we apply transformation (6) then the corresponding basic form becomes

$$g_5\left(x, \varphi; \kappa, \beta\right) = g_{\Phi|X}\left(\varphi|x; \beta\right) g_{5,X}\left(x; \kappa\right),$$

where

$$g_{5,X}\left(x; \kappa, \beta\right) \cong I_0\left(\beta\left(1 - x^2\right)\right) e^{\kappa x}, \qquad (11)$$

with the conditional density $g_{\Phi|X}$ given by (8). Furthermore, if $2\beta \leq \kappa$ the distribution is unimodal with the mode at $\widetilde{\underline{\mu}}_3$, which is the case Kent originally considered in [3]. If $2\beta > \kappa$ the distribution is bimodal, with modes at longitude $\varphi = 0$ and π, with the third coordinate, $\widetilde{x}_3$, defined by the equation $\cos\vartheta = \kappa/2\beta$ for both modes (Fig. 2).

Remark 4 All MATLAB scripts described in this paper are contained in the package **3D-Directional-SSV**.

When $2\beta \leq \kappa$, the parameters in this model have the meaning (see [3])

1. $|\kappa|$ represents the concentration
2. $\widetilde{\underline{\mu}}_3$ is the mean direction (pole or mode)
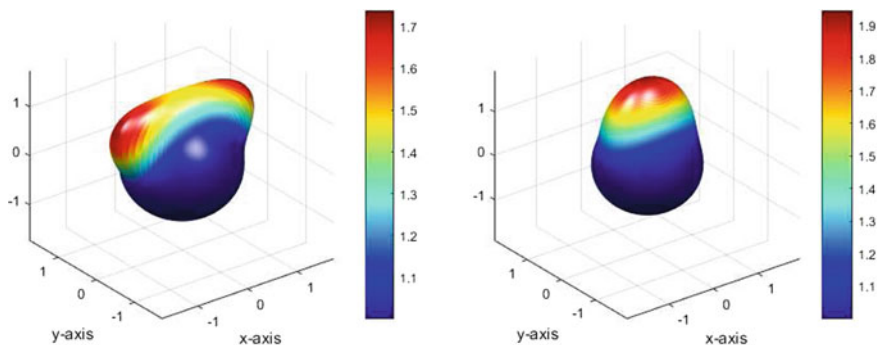
Fig. 2 Kent density, left: bimodal, $2\beta > \kappa$, modes are at $\vartheta = \pi/4$, and $\varphi = 0, \pi$; right: unimodal, $2\beta \leq \kappa$

3. $\widetilde{\underline{\mu}}_1$ and $\widetilde{\underline{\mu}}_2$ are, respectively, the major and minor axes of constant probability ellipses near the mode, and are determined only up to sign.

2.2.1 Equal-Area Projection and Separability of $\mathbf{FB}_6$

Equal-area projection of spherical densities provides the possibility of showing the simulations on a rectangle in the plane. As mentioned in [11], in the particular case when $2\beta \leq \kappa$, model $\mathbf{GFB}_{5,K}$ represents Lambert's equal-area projection of the sphere

$$y_1 = r\cos\varphi,\, y_2 = r\sin\varphi,\, r = \sin\left(\vartheta/2\right), \tag{12}$$

and separates the density (10) by coordinates y_1 and y_2. The inverse of this transform

$$\cos\vartheta = 1 - 2\left(y_1^2 + y_2^2\right),$$

$$\sin\varphi = \frac{y_2^2}{\sqrt{y_1^2 + y_2^2}},$$

$$\cos\varphi = \frac{y_1^2}{\sqrt{y_1^2 + y_2^2}}, \tag{13}$$

will be useful during simulations.

As shown in the Lemma below, the transformed Kent model $\mathbf{FB}_{5,K}$ can be written

$$f_5\left(y_1, y_2; \kappa, \zeta_1, \zeta_2\right) \cong e^{-2(\kappa-2\beta)y_1^2 - 4\beta y_1^4} e^{-2(\kappa+2\beta)y_2^2 + 4\beta y_2^4},$$

making the transformed coordinates independent. We show that the converse of this statement is also true.

Lemma 1 *Consider the model $\mathbf{FB}_6$ with density given in the form*

$$f_6\left(\widetilde{\underline{x}}; \kappa, \zeta_1, \zeta_2\right) \cong \exp\left(\kappa\widetilde{x}_3 + \sum_{k=1}^{3} \zeta_k\widetilde{x}_k^2\right). \tag{14}$$

The equal-area projection $f_6\left(y_1, y_2; \kappa, \zeta_1, \zeta_2\right)$ of (14) will be separable in y_1 and y_2 if only if $f_6\left(y_1, y_2; \kappa, \zeta_1, \zeta_2\right)$ corresponds to the Kent model $\mathbf{FB}_{5,K}$.

Proof Let us start from the $\mathbf{FB}_6$ density

$$f_6\left(\widetilde{\underline{x}}; \kappa, \zeta_1, \zeta_2\right) \cong \exp\left(\kappa\widetilde{x}_3 + \sum_{k=1}^{3} \zeta_k\widetilde{x}_k^2\right).$$

Now, apply the equal-area projection (12). We have

$$\widetilde{x}_3 = \cos \vartheta = 1 - 2r^2,$$
$$\widetilde{x}_1^2 = 4\left(1 - r^2\right) y_1^2,$$
$$\widetilde{x}_2^2 = 4\left(1 - r^2\right) y_2^2,$$
$$\widetilde{x}_3^2 = 1 - 4r^2\left(1 - r^2\right)$$

so that

$$f_6\left(y_1, y_2; \kappa, \zeta_1, \zeta_2\right) \cong \exp\left(-2\kappa r^2 + 4\left(1 - r^2\right)\left(\zeta_1 y_1^2 + \zeta_2 y_2^2 - \zeta_3 r^2\right)\right), \quad (15)$$

where $r^2 = y_1^2 + y_2^2$. Now, the exponent in details writes

$$- 2\kappa\left(y_1^2 + y_2^2\right) + 4\zeta_1 y_1^2 + \zeta_2 y_2^2 - \zeta_3\left(y_1^2 + y_2^2\right)$$
$$- 4\zeta_1\left(y_1^4 + y_1^2 y_2^2\right) - 4\zeta_2\left(y_2^4 + y_1^2 y_2^2\right) + 4\zeta_3\left(y_1^4 + 2y_1^2 y_2^2 + y_2^4\right).$$

The density (15) will be separable in y_1 and y_2 iff

$$\zeta_1 + \zeta_2 - 2\zeta_3 = 0. \qquad (16)$$

The sum $\zeta_1 + \zeta_2 - 2\zeta_3$ is invariant under the transformation (2), therefore setting $\zeta = (\zeta_1 + \zeta_2)/2$ in (2), (16) implies and implied by $\gamma = \zeta_3 - (\zeta_1 + \zeta_2)/2 = 0$, resulting in the Kent model $\mathbf{FB}_{5,K}$. $\qquad \square$

2.3 Bingham Model GFB$_{5,B}$

An alternate way to reduce the number of parameters by one in (5), is by setting $\kappa = 0$. This yields the density, with the canonical form

$$f_B\left(\underline{\widetilde{x}}; \beta, \gamma\right) \cong e^{\gamma \widetilde{x}_3^2 + \beta\left(\widetilde{x}_1^2 - \widetilde{x}_2^2\right)} = e^{\gamma \cos^2 \vartheta + \beta \sin^2 \vartheta \cos 2\varphi}. \qquad (17)$$
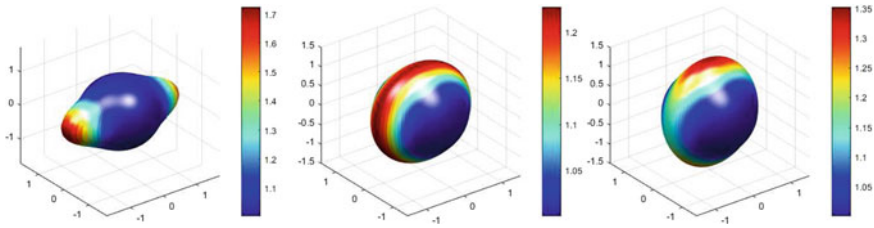
Application of transformation (6) gives the basic form

$$g_B\left(x, \varphi; \beta, \gamma\right) = g_{\Phi|X}\left(\varphi|x; \beta\right) g_{B,X}\left(x; \gamma\right),$$

where

$$g_{B,X}\left(x, \beta, \gamma\right) \cong I_0\left(\beta\left(1 - x^2\right)\right) e^{\gamma x^2},$$

see (8) for the conditional density $g_{\Phi|X}$, and recall the definition of the function I_0

$$I_0\left(\beta\left(1 - x^2\right)\right) = \int_0^{2\pi} e^{\beta\left(1 - x^2\right)\cos 2\varphi} d\varphi.$$

Fig. 3 Bingham model; $\beta = 3.2$, for all cases, $\gamma = -1.1 < \beta$, $\gamma = 3.2 = \beta$ and $\gamma = 4.1 > \beta$ from left to right respectively, here $\widetilde{\underline{\mu}} = (0, 0, 1)^\top$, and $\psi = 0$

Here, the marginal density $g_{B,X}$ contains the expression $\exp\left(\gamma x^2\right)$ which corresponds to the DW distribution, defined in Eq. (19).

Remark 5 In the particular case when $\beta = \gamma$, the density (17) has the form

$$f_B\left(\widetilde{\underline{x}}; \beta, \gamma\right) \cong e^{\gamma \widetilde{x}_3^2 + \beta\left(\widetilde{x}_1^2 - \widetilde{x}_2^2\right)} \cong e^{-2\gamma \widetilde{x}_2^2}. \tag{18}$$

This model (18) is a rotation of the DW model (see Eq. (19)) with negative parameter (we remind the reader that $\beta > 0$) and therefore (18) is a girdle distribution over the main circle $\widetilde{x}_2 = 0$.

If we fix β and change γ, there are three possible alignments: when $\gamma < \beta$ then it is bipolar with modal direction toward the x-axis, when $\beta = \gamma$ then it is girdle distribution, and finally when $\beta < \gamma$ then the modal direction becomes the north pole $\underline{\widetilde{N}}$. These are illustrated in Fig. 3.

2.4 Model GFB$_{4,\beta}$

We now consider the simplest form when the conditional density $g_{\Phi|X}$ is not constant, namely when the Θ and Φ are not independent random variables. Setting either $\kappa = 0$ and $\gamma = 0$ in (5), or $\kappa = 0$ in (9), or $\gamma = 0$ in (17), we get the density function which is a four-parameter family of distributions with canonical form

$$f_\beta\left(\widetilde{\underline{x}}; \beta\right) \cong e^{\beta\left(\widetilde{x}_1^2 - \widetilde{x}_2^2\right)} = e^{\beta \sin^2 \vartheta \cos 2\varphi}.$$

The basic form

$$g_\beta\left(x, \varphi; \beta\right) \cong e^{\beta\left(1 - x^2\right) \cos 2\varphi}$$

coincides formally with the conditional density $g_{\Phi|X}$. Nevertheless, the marginal density is not uniform since

$$g_\beta\left(x, \varphi; \beta\right) = g_{\Phi|X}\left(\varphi|x; \beta\right) g_{\beta,X}\left(x, \beta\right)$$

where

$$g_{\beta,X}(x,\beta) \cong I_0\left(\beta\left(1-x^2\right)\right),$$

and $g_{\Phi|X}$ follows a vMF distribution on the circle as we have already mentioned (see (8)).

2.5 Model GFB$_4$

Setting $\beta = 0$, in (5) we reduce the number of parameters by two (β, and angle ψ) resulting in the canonical form

$$f_4\left(\widetilde{\underline{x}};\kappa,\gamma\right) \cong e^{\kappa\widetilde{x}_3+\gamma\widetilde{x}_3^2} = e^{\kappa\cos\vartheta+\gamma\cos^2\vartheta}.$$

This density does not depend on longitude φ. Instead, it depends only on $\cos\vartheta$ and hence, is rotationally symmetric (see Lemma 4 in [1]). Note that this model as well as (19) below are indeed generalized von Mises ones (for which simulation algorithms are well-studied) since $\cos^2(x) = (1 + \cos(2x))/2$.

Transformation (6) provides the basic form

$$g_4(x;\kappa,\gamma) \cong e^{\kappa x+\gamma x^2}.$$

A particular case of Model GFB$_4$ when $\kappa = 0$, is the following three-parameter family:

2.6 Dimroth-Watson Model GFB$_{3,DW}$

The Dimroth-Watson Distribution (DW) [12] distribution is given by the density function

$$f_W\left(\widetilde{\underline{x}};\gamma,\underline{\widetilde{\mu}}\right) = \frac{1}{M\left(1/2, 3/2, \gamma\right)}e^{\gamma\left(\underline{\widetilde{\mu}}\cdot\underline{\widetilde{x}}\right)^2} = \frac{1}{M\left(1/2, 3/2, \gamma\right)}e^{\gamma\cos^2\vartheta}, \qquad (19)$$

where $M\left(1/2, 3/2, \gamma\right)$ is Kummer's function (not to be confused with the orthogonal matrix M described above) and where $\vartheta = \arccos\left(\underline{\widetilde{\mu}}\cdot\underline{\widetilde{x}}\right)$, (see [1]). Either setting $\gamma = 0$, in Model GFB$_4$, or $\beta = 0$ in the Kent Model GFB$_{5,K}$, we arrive at the most basic model on the sphere viz. the von Mises–Fisher distribution.
Model GFB$_{3,vMF}$

The widely used von Mises–Fisher Model (vMF) density is given by

$$f_{\text{vMF}}\left(\underline{\widetilde{x}}; \kappa, \underline{\widetilde{\mu}}\right) = \frac{\sqrt{\kappa}}{(2\pi)^{3/2} I_{1/2}(\kappa)} e^{\kappa \underline{\widetilde{\mu}} \cdot \underline{\widetilde{x}}}, \quad (20)$$

with basic form

$$g_{\text{vMF}}(x; \kappa) = \frac{\sqrt{\kappa}}{(2\pi)^{3/2} I_{1/2}(\kappa)} e^{\kappa x}.$$

3 A Spherical Histogram

A histogram for a random sample on the unit sphere $\mathbb{S}_2$ usually assumes an equal-area discretization of the sphere. We now discuss an alternative, viz. the **HEALPix** (**H**ierarchical, **E**qual **A**rea and iso**L**atitude **Pix**elization) discretization, a detailed description of which can be found in [13]. In the first step of the pixelization the sphere is partitioned into 12 equal-area spherical quadrilaterals (pixels), and in each subsequent step, all the existing pixels are divided into 4 equal-area quadrilaterals. HEALPix is a discretization with the resolution parameter n_{side} (number of steps of division, which is a power of 2) and total number of pixels equal to $n_{\text{pix}} := 12n_{\text{side}}^2$ such that $\sum_{k=1}^{n_{\text{pix}}} n_k = n$, and each with an area of $4\pi/n_{\text{pix}}$.

If we are given a random sample $\underline{\widetilde{X}}_j$, $j = 1, 2, \ldots n$, on the sphere $\mathbb{S}_2$, then for each pixel/ quadrilateral Π_k, $k = 1, 2, \ldots n_{\text{pix}}$ we set an integer n_k which counts the number of the sample elements contained in the pixel Π_k. We use the nested numbering scheme for ordering pixels, where Π_k is the kth pixel according to this scheme. The nested scheme is appropriate for decreasing the resolution, since one can easily accumulate the samples included in 4 "neighboring" pixels.

We define the histogram $H\left(\underline{\widetilde{x}}\right)$ such that it is constant over a quadrilateral Π_k and the integral over the sphere is 1:

$$H\left(\underline{\widetilde{x}}\right) = \frac{n_{\text{pix}} n_k}{4\pi n}, \quad \underline{\widetilde{x}} \in \Pi_k.$$

We plot the histogram drawing a column with height $n_{\text{pix}} n_k / 4\pi n$ over each quadrilateral. For instance, let $\widetilde{X}_j$, $j = 1, 2, \ldots n = 2^{12}$, be a random sample from the uniform distribution and $n_{\text{side}} = 2^3$, so that $n_{\text{pix}} = 768$. We plot the sample and the corresponding histogram in Fig. 4.

An important feature of this histogram lies in the plot construction. Mathematically, when the columns from each quadrilateral are extruded from the surface of the sphere, the height is measured normal to the center of the pixel, and the volume is given as the height times the area of the quadrilateral as described above, as expected. However, graphically we also extrude all of the pixel edges normal to their respective location on the sphere. This results in taller columns having larger patches and shorter columns having smaller patches at their respective termini, and stands that maintain pixel surface area at all elevations, which forces adjacent columns
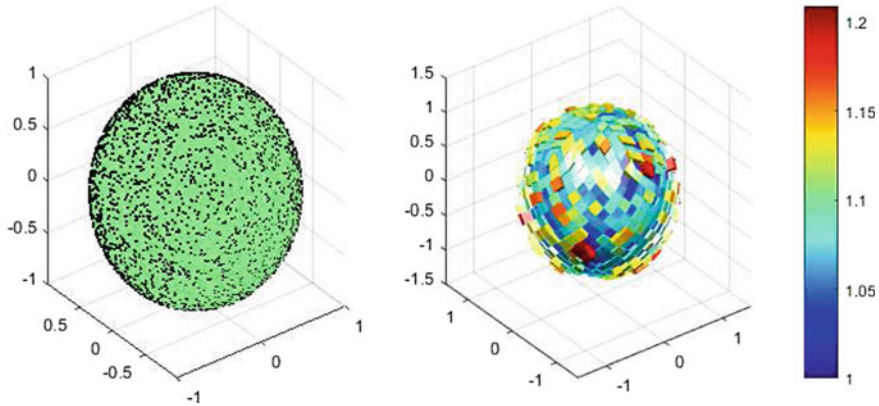
Fig. 4 Uniform sample and its histogram

to become increasingly separated as column height increases, and results in a *pin cushion* type histogram.

4   Simulation of Random Variates on the Sphere

All the simulations described here will have some common features and these are the following:

1. We start with the case $\kappa \geq 0$ in formulae, but also allow for the case $\kappa \leq 0$ during simulation. We simulate a random variate $\widetilde{X}$ with $|\kappa|$ and as a final step (but before rotation) change the variate $\widetilde{X}$ to $-\widetilde{X}$ (see Remark 1).

2. All algorithms below concern the case when the frame of reference is xyz, with the modal/mean direction as the north pole, i.e., $\widetilde{\mu} = \widetilde{N}$.

3. The plots are generated by the following parameters: Sample size is $n = 2^{12} = 8192$, resolution of the discretized sphere $\mathbb{S}_2$ is $n_{\text{side}} = 2^3$, which yields a total pixel count of $n_{pix} = 768$. The resolution for theoretical density plots is 101×101 of the set of angles $(\vartheta, \varphi) \in [0, \pi] \times [0, 2\pi]$.

4. We characterize a rotation corresponding to $M = \left[\widetilde{\mu}_1, \widetilde{\mu}_2, \widetilde{\mu}_3 \right]$ by a vector $\widetilde{\mu}$ and an angle ψ, such that $\widetilde{\mu}_3$ represents $\widetilde{\mu}$, and $\widetilde{\mu}_1, \widetilde{\mu}_2$ define the angle ψ, see Sect. 2.1 for details. When an angle of a random variate is changed by ψ, then the corresponding density is changes by $-\psi$.

4.1 Acceptance-Rejection Method

For the simulation of random variates from various distributions discussed here, we make frequent use of the standard acceptance-rejection method. For a detailed account of this classic simulation technique see, e.g., [14] and [15], but a general overview of this method for any particular distribution is as follows.

We wish to sample random variate X from a target distribution with density $f_X(x)$ (given up to a constant multiplier) which can be evaluated for any x, for which the simulation process is either exceptionally difficult, or perhaps even unknown. Because $f_X(x)$ can be computed, we can write the density $f_X(x) = cg(x)h(x)$, where the constant $c \geq 1, 0 < g(x) \leq 1$, and $h(x)$ is a probability density function from which we know how to sample.

The algorithm is based on checking the inequality $U \leq g(Y)$, where U is uniform on the interval $(0, 1)$, and if it is satisfied, then Y will be accepted as a random variate from $f_X(x)$.

In practice, we seek a density $h(x)$ such that

$$f_X(x) \leq c_1 h(x),$$

where $c_1 \geq 1$, then set $g(x) = f_X(x)/c_1 h(x)$ and call the denominator as the *envelope*. To maximize algorithmic efficiency, the acceptance ratio $1/c_1$ should be maximized such that the constant c_1 is as close to one as possible, which naturally depends on the choice of density $h(x)$.

If $\widetilde{f}_X$ coincides with f_X except some constant c_f, $f_X \cong \widetilde{f}_X$, and similarly $\widetilde{h}$ coincides with h except some constant c_h, $h_X \cong \widetilde{h}_X$, and $\widetilde{f}_X \leq \widetilde{h}$, then

$$c_f \widetilde{f}_X(x) = f_X(x) \leq c_f \widetilde{h}(x) = \frac{c_f}{c_h} c_h \widetilde{h}(x) = c_1 h(x),$$

where $1/c_1 = c_h/c_f$ is the acceptance ratio. Therefore the test can be performed by checking the inequality

$$U \leq g(Y) = \frac{f_X(Y)}{c_1 h(Y)} = \frac{\widetilde{f}_X(Y)}{\widetilde{h}(Y)}, \tag{21}$$

where again Y and U are distributed by $h(y)$ and uniform respectively. This method has been used extensively by Wood [2, 16]. In particular Ulrich [17] discusses a general method for simulating a rotationally symmetric variable. We employ this technique in different contexts.

4.2   Simulation of FB Families

We shall describe the simulation of the canonical variates. The necessary rotation can be done separately in each case and is included in the appropriate scripts of the MATLAB package **3D-Directional-SSV**.

   We shall use the well-known basic algorithms for simulation of spherical uniform, vMF and DW random variates (Suppl., Alg. 3–6).

   The inequality (21) shows that for the simulation we do not need the normalizing constants, although they are needed for calculating the acceptance ratios. If these constants are not available analytically, we use numerical integration for calculating the acceptance ratios.

4.2.1   Model GFB$_4$

GFB$_4$ generalizes both the vMF and DW models. We use the envelopes proposed by Wood [2] in the application of acceptance-rejection sampling as described above.

   The density in basic form

$$g_4 (x; \kappa, \gamma) \cong e^{\kappa x + \gamma x^2},$$

implies that the longitude $\Phi = 2\pi U$, where U is uniformly distributed independently of the colatitude Θ, and hence we concentrate on simulating $X = \cos \Theta$. Also, we assume that the parameters κ and γ are not identically zero, because otherwise the model is simplified to either the vMF or DW. We consider three cases depending on the relation between the parameters κ and γ.

1. If $\gamma < 0, 0 \leq \kappa \leq -2\gamma$, complete the quadratic form in the exponent and rewrite g_4 as

$$g_4 (x; \kappa, \gamma) \cong e^{\gamma (x + \kappa/2\gamma)^2}, \ x \in [-1, 1],$$

   and use the Gaussian envelope. The acceptance ratio is large if we assume that the mean $-\kappa/2\gamma$ belongs to the interval $[-1, 1]$, which is the case under this assumption.
2. If $\gamma < 0, \kappa \geq -2\gamma$, then we use vMF $g_{vMF} (x, \kappa + 2\gamma)$ on $\mathbb{S}_2$, as an envelope.
3. If $\gamma > 0$, an envelope composed of a mixture of $g_{vMF} (x, \kappa + \gamma)$ and $g_{vMF} (x, \kappa - \gamma)$ vMF distributions is used.

   The difference between our method and the one described in [2], is how we partition the case where $\gamma < 0$.[1]

   Some particular cases with interesting features arise in the simulation of models in the **GFB**$_5$ family. In this vein, we consider **GFB**$_{4,\beta}$, which demonstrates the difficulty

---

[1] Note: In [2], the Procedure for FB$_4^-$ on p.890 has a misprint. The correct expressions should be $\mu_1 = (2\gamma - \kappa)/\sqrt{-2\gamma}, \quad \mu_2 = -(2\gamma + \kappa)/\sqrt{-2\gamma}$.

of combining two algorithms, as well as the problem of simulation of Φ according to the conditional density $g_{\Phi|X}$.

4.2.2   Model GFB$_{4,\beta}$

If $\beta \neq 0$, $\gamma = 0$, $\kappa = 0$, the density in basic form is given by

$$g_\beta \left(x, \varphi; \kappa, \beta \right) \cong e^{\beta\left(1-x^2\right) \cos 2\varphi},$$

and has marginal

$$g_{\beta,X} \left(x, \beta \right) \cong I_0 \left(\beta \left(1 - x^2 \right) \right),$$

and conditional $g_{\Phi|X}$, see (8), densities.

The simulation of the marginal X is based on the inequality

$$\frac{1}{c_I} I_0 \left(\beta \left(1 - x^2 \right) \right) \leq \frac{c}{2c_I} \left(p_1 f_W \left(x; -\beta \right) + p_2 f_W \left(x; \beta \right) \right)$$

where

$$c_I = \int_{-1}^{1} I_0 \left(\beta \left(1 - x^2 \right) \right) dx.$$

With the mixture of two DW densities, one is bipolar when the parameter β in f_W is positive and the other one is a girdle distribution.

Now, we use the acceptance-rejection method for the simulation of $X = \cos \Theta$, with an acceptance ratio of $2c_I/c$ that is decreasing as β is increasing (see Fig. 5).

The simulation of longitude Φ according to the conditional density $g_{\Phi|X}$ is given by simulating 2Φ as a vMF distributed random variate on $\mathbb{S}_1$ (see Remark 3). It yields a value in $[0, \pi]$, and hence, Φ itself will be an element in $[0, \pi/2]$. The density function g_β has the same value at Φ, $-\Phi$, $\Phi + \pi$, and $-\Phi + \pi$, therefore we shall extend the simulated value randomly.
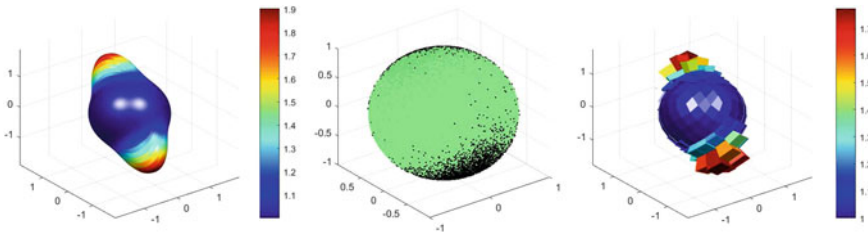

Fig. 5   Model **GFB**$_{4,\beta}$

4.2.3   Model GFB$_{5,K}$

Here we consider the Kent model **GFB**$_{5,K}$, and note that the equal-area projection simplifies the problem to one of simulating two independent random variates.[2]
Equal-area projection, case $2\beta \le \kappa$

This part of the simulation of the Kent model **GFB**$_{5,K}$

$$f_5\left(\widetilde{\underline{x}}; \kappa, \beta\right) \cong e^{\kappa \widetilde{x}_3 + \beta\left(\widetilde{x}_1^2 - \widetilde{x}_2^2\right)},$$

has been considered by Kent [11] under the assumption,

$$0 \le 2\beta \le \kappa. \tag{22}$$

This is the case when the exponent of the density is a nonincreasing function of ϑ for each φ, and when the model is unimodal (see Fig. 6). The Kent model, **GFB**$_{5,K}$, under transformation (12) has the form

$$f_5\left(y_1, y_2; \kappa, \beta\right) \cong e^{-2(\kappa-2\beta)y_1^2 - 4\beta y_1^4} e^{-2(\kappa+2\beta)y_2^2 + 4\beta y_2^4},$$

which is a product of two densities. Introduce

$$\alpha_1 = \kappa - 2\beta, \quad \alpha_2 = \kappa + 2\beta,$$

in this parametrization the density has the form

$$f_5\left(y_1, y_2; \kappa, \beta\right) \cong e^{-2\alpha_1 y_1^2 - 4\beta y_1^4} e^{-2\alpha_2 y_2^2 + 4\beta y_2^4}. \tag{23}$$

If assumption (22) holds then

$$\alpha_1 \ge 0, \quad \alpha_2 \ge 0,$$

and we use Kent's algorithm [11].
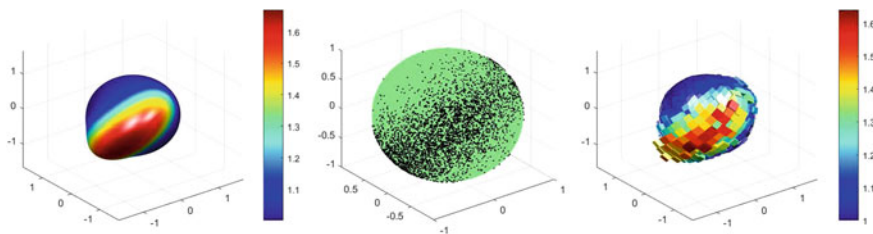
Fig. 6   Model **GFB**$_{5,K}$, unimodal: $2\beta \le \kappa$, from left to right: density, sample, histogram

---

[2] See Sect. 2.2.1 for details.

We simplify Kent's algorithm, using a Gaussian envelope instead of the exponential envelope. From Kent's method, we stop at the first inequality and apply the acceptance-rejection method right there. The basic inequality is given by,

$$-\frac{1}{2}\delta^2 w^2 \le \frac{1}{2}\tau^2 - \delta\tau\,|w|, \quad \delta, \tau > 0.$$

Setting $\delta = \sqrt{8\beta}$, and $\tau = 1$, we have

$$\exp\left(-2\alpha_1 y_1^2 - 4\beta y_1^4\right) \le \exp\left(\frac{1}{2} - \frac{1}{2}\left(4\alpha_1 + \sqrt{8\beta}\right) y_1^2\right),$$

which gives the Gaussian envelop with variance $\sigma_1^2 = 1/\left(4\alpha_1 + \sqrt{8\beta}\right)$. Similarly

$$\exp\left(-2\alpha_2 y_2^2 + 4\beta y_2^4\right) \le \exp\left(-\frac{1}{2}\left(4\alpha_2 - 8\beta\right) y_2^2\right),$$

yields a Gaussian envelop as well, with variance $\sigma_2^2 = 1/4\kappa$.[3] We combine these two and use acceptance-rejection method.

Equal-area projection, case $2\beta > \kappa$

We are also interested in the case when the density increasing and decreasing in ϑ around $\varphi = 0$.

$$0 \le \kappa \le 2\beta,$$

In this case,

$$\alpha_1 = \kappa - 2\beta \le 0,$$
$$\alpha_2 = \kappa + 2\beta \ge 0.$$

Let us start with the first component of (23), $\exp\left(-2\alpha_1 y_1^2 - 4\beta y_1^4\right)$. The polynomial

$$p(y_1) = -\alpha_1 y_1^2 - 2\beta y_1^4,$$

in the exponent is symmetric to zero. We restrict the variable y_1 such that $|y_1| \le 1$, hence we have two maximums at $y_0 = \pm\sqrt{(1 - \kappa/2\beta)/2}$, where

$$p(y_0) = \frac{\beta}{2}\left(1 - \frac{\kappa}{2\beta}\right)^2.$$

Therefore we separate the interval $[-1, 1]$ and use Gaussian envelope

$$\exp\left(-2\alpha_1 y_1^2 - 4\beta y_1^4\right) \le \exp\left(-2\left(\frac{\beta}{2}\left(1 - \frac{\kappa}{2\beta}\right)(y_1 - y_0^+)^2 + p(y_0)\right)\right), \quad (24)$$

---

[3] Our algorithm corrects an error in [11].

on [0, 1]. This envelope will exactly match the target density at the maximum; otherwise it is greater.

Similarly

$$\exp\left(-2\alpha_2 y_2^2 + 4\beta y_2^4\right) \leq \exp\left(-\left(2\alpha_2 - 4\beta\right)y_2^2\right) = \exp\left(-2\kappa y_2^2\right), \quad (25)$$

provide a Gaussian envelop as well, with variance $\sigma_2^2 = 1/4\kappa$.

If $2\beta > \kappa$, then the model is bimodal, but not bipolar, and the cosine of the angle, η, between the modal directions is $\cos\eta = \kappa/2\beta$. We put $\kappa/2\beta = 1/2$, and hence $\eta = \pi/3$ (see Fig. 7).

4.2.4 Model GFB$_6$

The Kent model $\mathbf{GFB}_{5,K}$ and the Bingham Model $\mathbf{GFB}_{5,B}$ are included here since, as we shall see, there is only a small difference whether $\kappa = 0$, or $\gamma = 0$. If $\kappa = 0$, we pay particular attention to the case $\gamma = \beta \neq 0$, (see Remark 5).

We repeat the method applied for the FB$_\beta$, $\beta \neq 0$, with κ and γ, then we use a mixture of two FB$_4$ densities (Fig. 8).
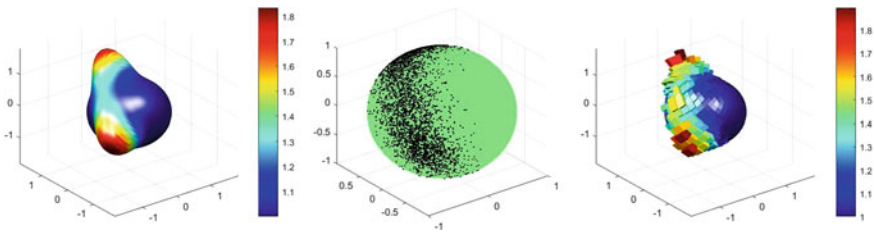

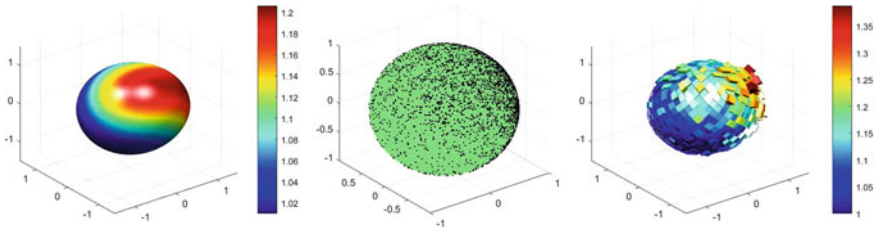**Fig. 7** If $2\beta > \kappa$, then the model $\mathbf{GFB}_{5,K}$, is bimodal

Fig. 8 Model $\mathbf{GFB}_6$, $\kappa = 1.5$; $\beta = 0.61$; $\gamma = 0.31$; $\mu = [1, -1, 1]$, $\psi = 0$

4.3 Simulating Spherical Distributions Resulting from Spherical Harmonics

As discussed in [1], if a density $f\left(\widetilde{x}\right)$ is continuous then it has a series expansion in terms of the spherical harmonics Y_ℓ^m,

$$f\left(\widetilde{x}\right) = \sum_{\ell=0}^{\infty} \sum_{m=-\ell}^{\ell} a_\ell^m Y_\ell^m\left(\widetilde{x}\right). \tag{26}$$

The coefficients $\left\{a_\ell^m\right\}$ may be considered as analogous to the characteristic function, they are complex valued with $a_\ell^{m*} = (-1)^m\, a_\ell^{-m}$, and are given by

$$a_\ell^m = \int_{\mathbb{S}_2} f\left(\widetilde{x}\right) Y_\ell^{m*}\left(\widetilde{x}\right) Q\left(d\widetilde{x}\right). \tag{27}$$

The notation $*$ is defined as the transpose and conjugate of a matrix and just the conjugate for a scalar. Several symmetries of distributions are characterized in terms of the coefficients a_ℓ^m given in (27).

For a detailed account of Spherical Distributions and Harmonic Analysis the reader is referred to [1], where the first few spherical harmonics are listed. Notice in particular, that the spherical harmonic $Y_0^0 = 1/\sqrt{4\pi}$, and hence $a_0^0 = 1/\sqrt{4\pi}$ is the normalizing constant for $f\left(\widetilde{x}\right)$ and $Q\left(d\widetilde{x}\right) = \sin\vartheta\, d\vartheta\, d\varphi$ is the Lebesgue element of surface area on $\mathbb{S}_2$.

Let $\widetilde{x}\left(\vartheta, \varphi\right)$ be a point on the unit sphere $\mathbb{S}_2$, then the spherical harmonics are defined by

$$Y_\ell^m\left(\vartheta, \varphi\right) = (-1)^m \sqrt{\frac{2\ell+1}{4\pi}\frac{(\ell-m)!}{(\ell+m)!}} P_\ell^m\left(\cos\vartheta\right) e^{im\varphi},\ \varphi \in [0, 2\pi],\ \vartheta \in [0, \pi],$$

where P_ℓ^m denotes *associated normalized* **Legendre function** *of the first kind.*

Real-valued spherical harmonics. Spherical harmonics are, in general, complex valued, due to the dependence of longitude φ given by $e^{im\varphi}$. Now, $e^{im\varphi}$ is a complete orthogonal system on the circle which is equivalent to the sine-cosine system for real-valued functions. Similarly, real-valued spherical harmonic functions are defined as

$$Y_{\ell,m} = \begin{cases} \frac{1}{\sqrt{2}}\left(Y_\ell^m + (-1)^m\, Y_\ell^{-m}\right) & m > 0 \\ Y_\ell^m & m = 0 \\ \frac{1}{i\sqrt{2}}\left(Y_\ell^{-m} - (-1)^m\, Y_\ell^m\right) & m < 0 \end{cases} \tag{28}$$

The harmonics of order $m > 0$ are said to be of the cosine type, and those with $m < 0$ of the sine type (Fig. 9).
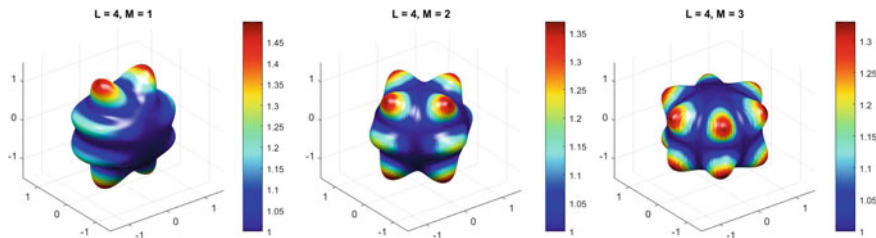
Fig. 9 Square of real spherical harmonics $Y_{4,m}^2$ with $L = 4$, $m = 1, 2, 3$

One may plot densities according to modulus square of complex and real spherical harmonics for any given L and all $m \in [-L, L]$ by the command $dx =$Density_SphHarm_All(L, m, real, resolution); if $m \notin [-L, L]$ then all $Y_{L,m}^2$ will be plotted, see our MATLAB package **3D-Directional-SSV** for details.

Example 1 Exponential family class of distributions [12],

$$g\left(\widetilde{\underline{x}}\right) = \exp \sum_{\ell=0}^{M} \sum_{m=-\ell}^{\ell} b_{\ell}^{m} Y_{\ell}^{m}\left(\widetilde{\underline{x}}\right),$$

where $b_{\ell}^{m*} = (-1)^m b_{\ell}^{-m}$. The normalizing constant corresponds to b_0^0 and depends on the rest of the b_{ℓ}^{m} parameters, such that the integral is necessarily 1. The likelihood of observations often has this form. In the case of rotational symmetry around axis $\widetilde{\underline{x}}_0$

$$f_e\left(\widetilde{\underline{x}}\right) = \exp\left(\sum_{\ell=0}^{M} b_{\ell} P_{\ell}\left(\cos \vartheta\right)\right)$$

where ϑ is the angle between $\widetilde{\underline{x}}$ and $\widetilde{\underline{x}}_0$, and P_ℓ denotes the *Standardized* Legendre polynomial ($P_0(x) = 1$).

Example 2 Another useful class of density functions is given by,

$$f\left(\widetilde{\underline{x}}\right) = \left|\sum_{\ell=0}^{\infty} \sum_{m=-\ell}^{\ell} d_{\ell}^{m} Y_{\ell}^{m}\left(\widetilde{\underline{x}}\right)\right|^2,$$

where $\sum_{\ell=0}^{\infty} \sum_{m=-\ell}^{\ell} \left|d_{\ell}^{m}\right|^2 = 1$. This class of distributions are of interest in, among other topics, the modeling of atoms.

In quantum mechanics, $Y_{\ell,m}\left(\widetilde{\underline{x}}\right)^2$ is considered as a probability density function, and plays an important role in the modeling of the hydrogen atom. The module square $\left|Y_{\ell}^{m}\left(\widetilde{\underline{x}}\right)\right|^2$ is also a density function that serves as an example of a rotational symmetric density function on the sphere, as it only depends on $\cos \vartheta$.

4.3.1   Simulation of Modulus-Square of Complex Harmonics

Consider the density $\left|Y_\ell^m\left(\widetilde{x}\right)\right|^2$ on $\mathbb{S}_2$ with respect to Lebesgue measure $\sin\vartheta\,d\vartheta\,d\varphi$. We have

$$\left|Y_\ell^m\left(\widetilde{x}\right)\right|^2 = \frac{2\ell+1}{4\pi}\frac{(\ell-m)!}{(\ell+m)!}P_\ell^m\left(\cos\vartheta\right)^2,$$

where P_ℓ^m is associated normalized Legendre function of the first kind.

$\left|Y_\ell^m\left(\widetilde{x}\right)\right|^2$ is rotational symmetric and $2\pi\left|Y_\ell^m\right|^2$ will be a density on $[-1,1]$. More precisely, the function

$$f_\ell^m\left(x\right) = c_\ell^m P_\ell^m\left(x\right)^2,$$

where

$$c_\ell^m = \frac{2\ell+1}{2}\frac{(\ell-m)!}{(\ell+m)!},$$

is a density on $[-1,1]$. We have $\left|Y_\ell^m\left(\widetilde{x}\right)\right|^2 = f_\ell^m\left(\cos\vartheta\right)^2/2\pi$. For convenience (MATLAB) we use the fully normalized associated Legendre function p_ℓ^m, such that $f_\ell^m\left(x\right) = p_\ell^m\left(x\right)^2$.

For general ℓ and m and $p_\ell^m\left(x\right)^2$, one can use Forsyth's method [18], with intervals defined by the zeros of $p_\ell^m\left(x\right)^2$ and Beta envelopes, say. In particular, let $\ell = 3$, $m = 2$. then $p_3^2\left(x\right)^2$ has a root at 0 and is symmetric around zero. For generating X, we apply the Neumann Theorem for $2f_3^2\left(x\right)$, since the Beta distribution with shape parameters $\alpha = 3.08$ and $\beta = 2.5249$, proved to be an efficient envelope for the density $2f_3^2\left(x\right)$.

The beta density is given by the function $b\left(x,\alpha,\beta\right) = x^{\alpha-1}\left(1-x\right)^{\beta-1}/B\left(\alpha,\beta\right)$, and the above shape parameters ($\alpha = 3.08$ and $\beta = 2.5249$) were found with the following steps:

1. let $\alpha, \beta > 1$,
2. use the relation $(\alpha-1)/(\alpha+\beta-2) = x_M$, between α and β, where x_M is the maximum point (modus) of $2f_3^2\left(x\right)$,
3. find the set of α and β under the (simultaneous) constraints:

    (i) $\max\limits_{x}\left(2f_3^2\left(x\right)/b\left(x,\alpha,\beta\right)\right) \geq 1$
    (ii) $\max\limits_{\alpha}\left(\min\limits_{x}\left(2f_3^2\left(x\right)/cb\left(x,\alpha,\beta\right)\right)\right) \leq 1$

4. choose a pair α and β, such that $\min\limits_{\alpha}\left(\max\limits_{x}\left(2f_3^2\left(x\right)/b\left(x,\alpha,\beta\right)\right)\right)$ is achieved.

We then have,

$$2f_3^2\left(x\right) = \frac{2f_3^2\left(x\right)}{b\left(x,\alpha,\beta\right)}b\left(x,\alpha,\beta\right)$$
$$= cg_3^2\left(x\right)h_3^2\left(x\right),$$

with $c = \max\left(2f_3^2\left(x\right)/b\left(x, \alpha, \beta\right)\right)$, $h_3^2\left(x\right) = b\left(x, \alpha, \beta\right)$, and $0 \leq g_3^2\left(x\right) = 2f_3^2\left(x\right)/$ $\left(cb\left(x, \alpha, \beta\right)\right) \leq 1$. We have found that $c = 1.074$, showing a high acceptance ratio.

4.3.2   Simulation of Real Harmonics $Y_{3,2}^2$

Consider the real spherical harmonic $Y_{3,2}$ given in (28). The density function $Y_{3,2}^2$ is given by

$$Y_{3,2}^2 = \frac{1}{2}\left(Y_3^2 + Y_3^{-2}\right)^2 = \frac{1}{2}\frac{7}{4\pi}\frac{1}{5!}P_3^2\left(\cos\vartheta\right)^2\left(e^{i2\varphi} + e^{-i2\varphi}\right)^2$$

$$= 2\sqrt{\frac{7}{4\pi}\frac{1}{5!}}P_3^2\left(\cos\vartheta\right)^2\cos^2 2\varphi.$$

This is a multimodal, non-rotationally symmetric distribution. The density function $Y_{3,2}^2$ is the multiplication of the density of Θ and the density of Φ respectively, which implies that the angles Θ and Φ are changing independently. The simulation of Θ according to the density $\cong P_3^2\left(\cos\vartheta\right)^2\sin\vartheta$, has been solved during the simulation of module square of complex harmonics above (Fig. 10).

The simulation of Φ by the density $\cong \cos^2\varphi$ is based on the following:

Let B be Beta distributed with $\alpha = 3/2$ and $\beta = 1/2$, and define $X = \arccos\left(\sqrt{B}\right)$. Then, from the equality

$$F_X\left(x\right) = P\left(\arccos\left(\sqrt{B}\right) \leq x\right) = P\left(B > \cos^2 x\right),$$

it follows 0

$$f_X\left(x\right) = 2f_B\left(\cos^2 x\right)\cos x\sin x$$

$$= \frac{2}{b\left(\alpha, \beta\right)}\left(\cos^2 x\right)^{1/2}\left(\sin^2 x\right)^{-1/2}\cos x\sin x = \frac{4\cos^2 x}{\pi} \qquad (29)$$

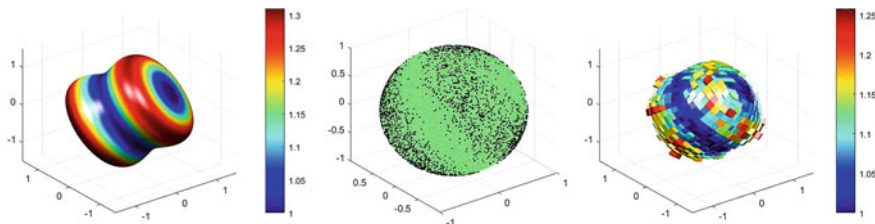Similarly, if B is a Beta distributed variate with $\alpha = 1/2$ and $\beta = 3/2$,

Fig. 10 Simulation of density $\left|Y_\ell^m\left(\widetilde{x}\right)\right|^2$

$$f_X(x) = 2f_B\left(\cos^2 x\right)\cos x \sin x$$

$$= \frac{2}{b(\alpha, \beta)}\left(\cos^2 x\right)^{-1/2}\left(\sin^2 x\right)^{3/2}\cos x \sin x = \frac{4\sin^2 x}{\pi}.$$

The latter of the two formulations for $f_X(x)$ is used for the simulation of $Y^2_{3,-2}$.

We conclude that the density of $\Phi = \arccos\left(\sqrt{B}\right)$ is $\cong \cos^2\varphi$, on $[-\pi/2, \pi/2]$. Once we have a random variate on $[-\pi/2, \pi/2]$ with density function depending on $\cos\varphi$ we can easily transform its values periodically to the interval $[0, 2m\pi]$, say. This works for the density

$$f\left(\widetilde{x}\right) \cong P^2_3\left(\cos\vartheta\right)^2\cos^2 2\varphi,$$

in this case we choose $m = 2$, since the longitude φ should have values on $[0, 2\pi]$, and we have the random variate 2Φ on $[-\pi/2, \pi/2]$. One can generalize this method for density $\cong \cos^2 k\varphi$, where k is any integer (Fig. 11).
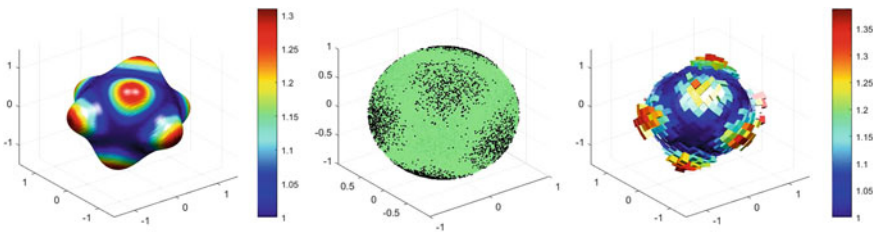
4.4 Simulation of a U-Distribution

Finally, we describe what we call the "$U-$distribution" (not to be confused with the uniform distribution), which provides a unique and interesting example of a spherical distribution that is antipodal, but not isotropic or rotationally symmetric.
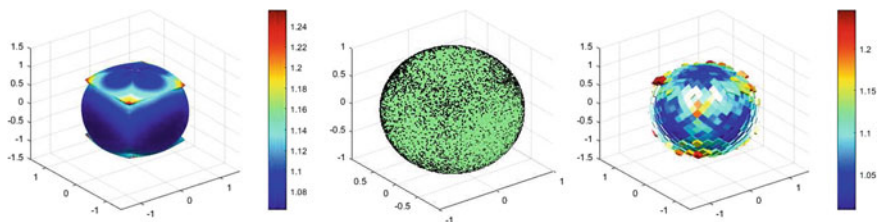
Consider U_1, U_2, U_3 that are independent uniform variables on $[0, 1]$. Then we define $\widetilde{\underline{Z}} = [Z_1, Z_2, Z_3] = (U_1, U_2, U_3)^\top / \sqrt{U_1^2 + U_2^2 + U_3^2}$, $\widetilde{\underline{Z}} \in \mathbb{S}_2$, and write

$$\widetilde{\underline{Z}} = (\sin\Theta\cos\Phi, \sin\Theta\sin\Phi, \cos\Theta).$$

We then have (Fig. 12)

Fig. 11 Simulation of density $Y^2_{3,2}$

Fig. 12 The U-distribution

$$\tan(\Phi) = \frac{Z_2}{Z_1} = \frac{U_2}{U_1}$$

$$P(\Phi < \varphi) = P\left(\frac{U_2}{U_1} < \tan(\varphi)\right)$$

$$= \begin{cases} \dfrac{\tan(\varphi)}{2} & \text{if } 0 \le \varphi < \pi/4 \\ 1 - \dfrac{1}{2\tan(\varphi)} & \text{if } \pi/4 \le \varphi < \pi/2 \end{cases},$$

and see mathematically that it is not the uniform density function

$$f_\Phi(\varphi) = \begin{cases} \dfrac{1}{2\cos^2(\varphi)} & \text{if } 0 \le \varphi < \pi/4 \\ \dfrac{1}{2\sin^2(\varphi)} & \text{if } \pi/4 \le \varphi < \pi/2, \end{cases}$$

Now, consider the conditional density $f_{\Theta|\Phi}(\vartheta|\varphi)$ for a fixed $\Phi = \varphi$,

$$\tan(\Theta)\cos(\Phi) = \frac{Z_1}{Z_3} = \frac{U_1}{U_3};$$

$$P(\Theta < \vartheta | \Phi = \varphi) = P\left(\frac{U_1}{U_3} < \cos(\varphi)\tan(\vartheta)\right)$$

$$= \begin{cases} \dfrac{\cos(\varphi)\tan(\vartheta)}{2} & \text{if } \varphi \in [0, \pi/4],\, \vartheta \in [0, \pi/2],\, \cos(\varphi)\tan(\vartheta) \le 1 \\ 1 - \dfrac{1}{2\cos(\varphi)\tan(\vartheta)} & \text{if } \varphi \in [0, \pi/4],\, \vartheta \in [0, \pi/2],\, \cos(\varphi)\tan(\vartheta) > 1 \end{cases},$$

$$f_{\Theta|\Phi}(\vartheta|\varphi)\,f_\Phi(\varphi)$$

$$= \begin{cases} \dfrac{\cos(\varphi)}{16\cos^2(\vartheta)\cos^2(\varphi)} & \text{if } \varphi \in [0, \pi/4]\,,\ \vartheta \in [0, \pi/2]\,,\ \cos(\varphi)\tan(\vartheta) \le 1 \\ \dfrac{1}{16\sin^2(\vartheta)\cos^3(\varphi)} & \text{if } \varphi \in [0, \pi/4]\,,\ \vartheta \in [0, \pi/2]\,,\ \cos(\varphi)\tan(\vartheta) > 1 \end{cases}.$$

References

1. Jammalamadaka, S. R., Terdik, G.: Harmonic analysis and distribution-free inference for spherical distributions. J. Multivariate Anal. **171**, 436–451 (2019)
2. Wood, A.T.A.: The simulation of spherical distributions in the Fisher-Bingham family. Commun. Stat.-Simul. Comput. **16**(3), 885–898 (1987)
3. Kent, J.T.: The Fisher-Bingham distribution on the sphere. J. Roy. Stat. Soc. Ser. B (Methodol.) 71–80 (1982)
4. Kent, J.T., Ganeiber, A.M., Mardia, K.V.: A new unified approach for the simulation of a wide class of directional distributions. J. Comput. Graph. Stat. **27**, 291–301 (2018)
5. Gatto, R.: The generalized von Mises–Fisher distribution. In: Advances in Directional and Linear Statistics: A Festschrift for Sreenivasa Rao Jammalamadaka, pp. 51–68. Springer Science & Business Media, Berlin (2011)
6. Mardia, K.V., Jupp, P.E.: Directional Statistics, vol. 494. Wiley, Hoboken (2009)
7. Fisher, R.A.: Dispersion on a sphere. Proc. Roy. Soc. Lond. A: Math. Phys. Eng. Sci. **217**(1130), 295–305 (1953)
8. Dimroth, E.: Untersiichungen aim wechanismiis von blastais und syntexis. Phylliterr and Hodelsen des siidm3lichen Fichtelgebirges I Die statistische Airswertung einfacher Giirteldiagranime Txheim Man Pctr Mitt. **8**, 248–274 (1962)
9. Watson, G.S.: Equatorial distributions on a sphere. Biometrika **52**(1/2), 193–201 (1965)
10. Bingham, C.: An antipodally symmetric distribution on the sphere. Ann. Stat. 1201–1225 (1974)
11. Kent, J.T., Hamelryck, T.: Using the Fisher-Bingham distribution in stochastic models for protein structure. Quant. Biol. Shape Anal. Wavelets **24**, 57–60 (2005)
12. Watson, G.S.: Statistics on Spheres. University of Arkansas Lecture Notes in the Mathematical Sciences, 6. Wiley, New York (1983)
13. Gorski, K.M., Hivon, E., Banday, A.J., et al.: HEALPix a framework for high-resolution discretization and fast analysis of data distributed on the sphere. Astrophys. J. **622**(2), 759 (2005)
14. von Neumann, J.: Various techniques used in connection with random digits. US Nat. Bur. Stand. Appl. Math. Ser. **12**, 36–38 (1951)
15. Rubinstein, R.Y.: Simulation and the Monte Carlo Method. Wiley, Hoboken (1981)
16. Wood, A.T.A.: Some notes on the Fisher-Bingham family on the sphere. Commun. Stat.-Theory Methods **17**(11), 3881–3897 (1988)
17. Ulrich, G.: Computer generation of distributions on the m-sphere. Appl. Stat. 158–163 (1984)
18. Atkinson, A.C., Pearce, M.C.: The computer generation of beta, gamma and normal random variables. J. Roy. Stat. Soc. Ser. A (General) 431–461 (1976)